J. Chem. Eng. Data **2007,** *52,* 941−947

Thermal Analysis and Calorimetric Study of 4-Dimethylaminopyridine

Quan Shi,[†,‡] Zhi-Cheng Tan,*[,†,§] You-Ying Di,[||] Bo Tong,[†,‡] Yan-Sheng Li,[§] and Shao-Xu Wang[§]

Thermochemistry Laboratory, Dalian Institute of Chemical Physics, Chinese Academy of Sciences, Dalian 116023, China, College of Chemistry and Chemical Engineering, Liaocheng University, Liaocheng 252059, China, College of Environmental Science and Engineering, Dalian Jiaotong University, Dalian 116028, China, and Graduate School of the Chinese Academy of Sciences, Beijing 100049, China

4-Dimethylaminopyridine (DMAP) is an important catalyst. The thermodynamic properties of DMAP were investigated through differential scanning calorimetry, thermogravimetric analysis, adiabatic calorimetry, and combustion calorimetry. The low-temperature heat capacity ($C_{p,\mathrm{m}}$) was measured in the temperature range from (80 to 402) K with a high-precision automated adiabatic calorimeter. The melting temperature (T_m), the molar enthalpy ($\Delta_\mathrm{fus}H_\mathrm{m}$), and the entropy ($\Delta_\mathrm{fus}S_\mathrm{m}$) of fusion were determined to be (387.094 ± 0.002) K, (21.628 ± 0.144) kJ·mol^{-1}, and (55.873 ± 0.372) J·K^{-1}·mol^{-1}, respectively. The mole fraction purity of the sample used in the adiabatic calorimetric study was determined to be 0.99964 according to the Van't Hoff equation. The thermodynamic functions $[H_T - H_{298.15}]$ and $[S_T - S_{298.15}]$ were derived in the range from (80 to 400) K with temperature interval of 5 K based on the heat capacity measurements. The constant-volume energy and standard molar enthalpy of combustion have been determined, $\Delta_\mathrm{c}U$ ($C_7H_{10}N_2$, cr) = −(4232.20 ± 0.60) kJ·mol^{-1} and $\Delta_\mathrm{c}H^0_\mathrm{m}$ ($C_7H_{10}N_2$, cr) = −(4235.92 ± 0.60) kJ·mol^{-1}, by means of a precision oxygen-bomb combustion calorimeter at T = (298.15 ± 0.001) K. The standard molar enthalpy of formation has been derived, $\Delta_\mathrm{f}H^0_\mathrm{m}$ ($C_7H_{10}N_2$, cr) = (52.20 ± 1.71) kJ·mol^{-1}, from the standard molar enthalpy of combustion in combination with other auxiliary thermodynamic quantities through a Hess thermochemical cycle.

Introduction

4-Dimethylaminopyridine (DMAP; molecular formula: $C_7H_{10}N_2$; CAS Registry No. 1122-58-3) belongs to the category of 4-position substitution derivatives of pyridine. It is widely used as a hypernucleophilic acylation catalyst.[1] Its molecular structure is as follows:

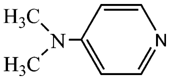

In the 1960s, DMAP was reported as a very effective acylation catalyst, and it accelerates the reaction rate by approximately 10^4 for the benzoylation of *m*-chloroaniline in comparison with pyridine.[2] As a result, DMAP has become one of the most popular catalysts for different processes such as acylations, alkylations, silylations, Baylis−Hillman reaction, catalytic microencapsulated polymers, and nucleophilic substitutions of alcohols, amines, phenols, and enolates.[3−6] DMAP may be considered as a potential candidate to replace typical anionic initiators used to homopolymerize epoxy monomers,[7,8] and it can also be used as a capping ligand for gold nanoparticles.[9,10] Moreover, the development of chiral DMAP derivatives has received considerable attention since they have been successfully employed as chiral nucleophilic catalysts in a wide range of asymmetric synthetic processes.[11−13] However, few studies on thermodynamic properties of DMAP are reported until now. In order to improve the process of chemical synthesis and increase understanding of this "supercatalyst", the study of thermodynamic properties for the substance is necessary.

In this paper, the thermal stability of DMAP was examined by thermogravimetry (TG) and differential scanning calorimetry (DSC). After that the thermodynamic properties were further carefully studied. The low-temperature heat capacity of the organic compound over the temperature range (80 to 402) K was measured by an automated adiabatic calorimeter. The standard molar enthalpies of combustion at T = 298.15 K were determined by oxygen-bomb combustion calorimetry.

Experimental Section

The sample of DMAP used in this study was purchased from ACROS ORGANICS Company. The labeled mole fraction purity is > 99.0 %. The sample was purified by recrystallizing it three times using ethanol with an analytical grade prior to the calorimetric experiments. The melting temperature of the sample was determined to be T = (386.7 to 387.9) K with a microscopic melting point device (model BY-1, Yazawa Co., Japan), and it is in agreement with the literature value, 387 K.[14,15] The structure of the sample was checked by IR (model 260-10, HITACHI Co., Japan), and ^{1}H NMR (model Unity Plus 500, Varian Ltd., UAS, $CDCl_3$), and the mole fraction purity was analyzed by HPLC (model LC-10AT, Japan) to be more than 99.8 %.

DSC analysis was carried out in a Setaram DSC-141 calorimeter. The sample mass about 0.00342 g was weighted into a closed aluminum pan, placed in the DSC cell, and heated at the rate of 5 K·min^{-1} under high-purity nitrogen atmosphere with a flow rate of 50 mL·min^{-1}. TG analysis was performed on Setaram Setsys 16/18 apparatus. A mass of 0.00613 g was

---

* Corresponding author. E-mail: tzc@dicp.ac.cn. Fax: +86-411-84691570. Tel: +86-411-84379199.

[†] Chinese Academy of Sciences.

[‡] Graduate School of the Chinese Academy of Sciences.

[§] Dalian Jiaotong University.

[||] Liaocheng University.

10.1021/je6005423 CCC: \$37.00

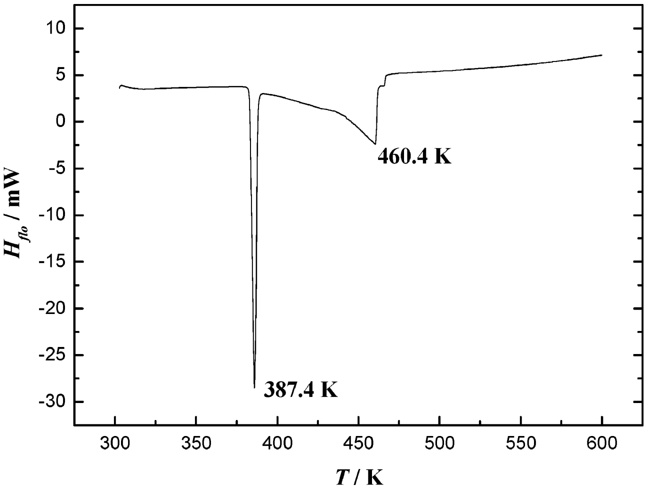

Figure 1. DSC curve of DMAP under high-purity nitrogen (99.999 %). H_{flo} is the heat flow.

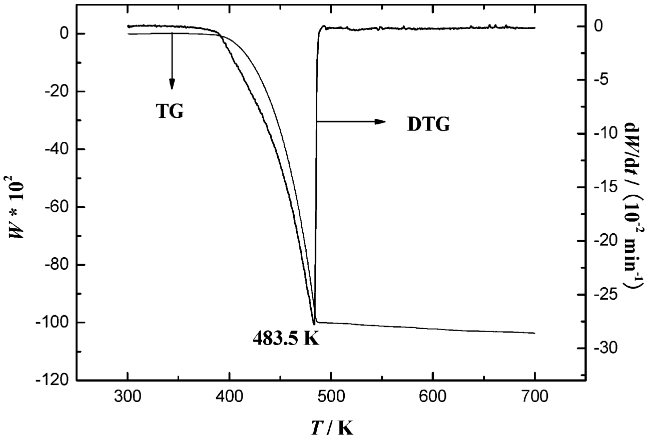

Figure 2. TG−DTG curves of DMAP under high-purity nitrogen (99.999 %). *W* is the mass lose of the sample in percent.

placed in a 100 μL α-alumina crucible and heated from room temperature to 723 K with a rate of 10 K·min^{-1} under high-purity nitrogen atmosphere with a flow rate of 60 mL·min^{-1}.

A precision automatic adiabatic calorimeter was applied to measure the heat capacities over the temperature range from (80 to 402) K. The calorimeter was established in Thermochemistry Laboratory of Dalian Institute of Chemical Physics, Chinese Academy of Sciences in the People's Republic of China. The principle and structure of the adiabatic calorimeter were described in detail elsewhere.[16−18] The sample amount used for the heat capacity measurement after buoyancy correction is 3.80308 g, which is equivalent to 31.129 mmol based on its molar mass of 122.17 g·mol^{-1}. The heating duration and temperature increment for each experimental heat capacity point were usually controlled to be about 10 min and (1 to 3) K, respectively, during the whole experimental process. Prior to the heat capacity measurements of the sample, the reliability of the calorimetric apparatus was verified by heat capacity measurements of the reference standard material, α-Al_2O_3. The sample mass used after buoyancy correction was 6.48265 g, which is equivalent to 63.580 mmol based on its molar mass of 101.9612 g· mol^{-1}. The deviations of our calibration results from those of the smoothed curve lie within ± 0.2 %, while the uncertainty is within ± 0.3 %, as compared with the recommended values reported by Archer[19] of NIST in the temperature range from (80 to 405) K.

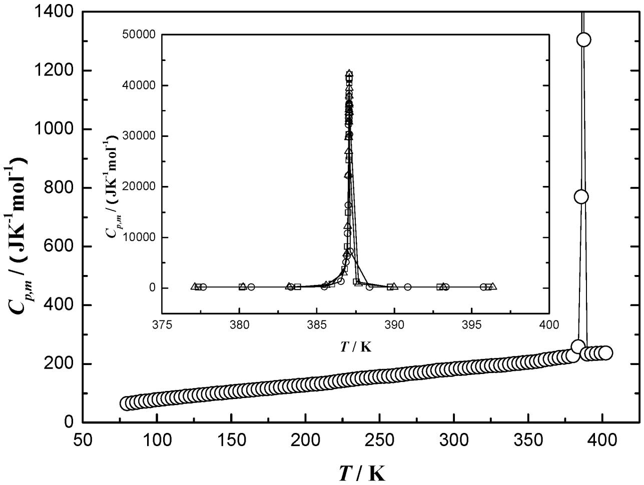

Figure 3. Experimental molar heat capacity $C_{p,\mathrm{m}}$ of DMAP as a function of temperature.

The constant-volume enthalpy of combustion was measured by means of a precision oxygen-bomb combustion calorimeter, which was an isoperibolic calorimeter with a static oxygen bomb. The calorimeter was set up in our thermochemistry laboratory, and the structure and principle of the calorimeter have been described previously in detail.[20−22] The sample (about 0.4 g) was pressed into pellets and put in a small sample crucible of about 0.004 dm^3, which was suspended in the bomb of about 0.3 dm^3, and burned under an oxygen pressure of 3.01 MPa ignited by a nickel fuse of about 16 cm in the presence of 0.0005 dm^3 of distilled water in the bomb to ensure equilibrium in the final state after the combustion. The purity of the oxygen used in the combustion was of research grade, mole fraction 0.99998. The real energy of combustion of the nickel fuse (Q_{Ni}) was calculated from the formula, $Q_{\mathrm{Ni}}/\mathrm{J} = 2.929 \cdot \Delta L$, in which ΔL/cm was the length of the combusted nickel wire. The energy of formation of the aqueous nitric acid produced by oxidation of a trace of nitrogen, which was contained in the oxygen bomb and was produced from the combustion reaction, was determined by the neutral titration with 0.08684 mol·dm^{-3} of sodium hydroxide solution by using phenolphthalein as the indicator. The enthalpy of formation of the aqueous nitric acid in the oxygen bomb can be derived from the equation, $Q_{\mathrm{HNO_3}}/\mathrm{J} = 59.8NV$, in which N/mol·dm^{-3} is the concentration of the sodium hydroxide solution and V/cm^3 is the volume of the consumed sodium hydroxide solution, based on the molar energy of formation of HNO_3(aq) from N_2(g), O_2(g), and H_2O(l). $\Delta_f H^0_m = 59.8$ kJ·mol^{-1},[23,24] for 0.1 mol·dm^{-3} of HNO_3(aq).

Results and Discussion

DSC and TG Analysis. Prior to adiabatic calorimetry and combustion calorimetry, thermal (phase) behavior of DMAP was obtained by DSC and TG. DSC curves are shown in Figure 1. Two endothermic peak appeared during the heating process with peak temperature, (387.4 and 460.4) K, which are ascribed to melting and evaporation respectively based on the previous measurements of melting temperature. The melting temperature was determined to be 387.1 K, which coincides with the literature value.[14,15] The molar enthalpy of fusion was determined to be 21.62 kJ·mol^{-1} by integration of the area of the first peak. The molar entropy of fusion was derived to be 55.85 J·K^{-1}·mol^{-1}. TG curves are shown in Figure 2. It can be seen that the mass loss was completed in a single step, reaching the maximum rate at $T = 483.5$ K. The mass loss is 100 % when the temperature reaches 500 K. The FT-IR spectrum of the

Table 1. Experimental Molar Heat Capacity Data of DMAP[a]

T/K	C_p/J·K^{-1}·mol^{-1}	T/K	C_p/J·K^{-1}·mol^{-1}	T/K	C_p/J·K^{-1}·mol^{-1}	T/K	C_p/J·K^{-1}·mol^{-1}	T/K	C_p/J·K^{-1}·mol^{-1}
				Series 1					
80.029	64.465	155.944	107.422	232.059	146.844	307.473	185.410	383.762	258.441
83.524	66.813	158.929	108.617	235.106	149.013	310.421	187.121	385.970	769.543
86.437	69.049	161.982	109.905	238.154	150.963	313.405	188.443	386.808	3811.059
89.410	71.035	165.100	111.539	241.183	152.052	316.419	189.786	386.971	8242.796
92.439	72.951	168.189	113.065	244.186	153.794	319.402	191.080	387.029	14935.247
95.511	74.900	171.249	114.493	247.179	155.152	322.402	192.541	387.051	25278.620
98.506	76.862	174.283	115.970	250.165	156.563	325.407	193.752	387.063	37788.286
101.434	78.683	177.291	117.203	253.132	157.383	328.415	194.698	387.069	35542.392
104.423	80.510	180.272	118.569	256.162	158.569	331.502	195.133	387.074	32855.468
107.476	82.302	183.322	120.194	259.236	159.801	334.532	196.953	387.079	30388.351
110.470	83.917	186.437	121.884	262.287	161.744	337.562	198.328	387.081	35886.974
113.409	85.666	189.533	123.230	265.401	163.214	340.666	200.842	387.088	40504.228
116.409	87.309	192.600	124.432	268.514	165.517	343.661	201.985	387.091	41155.447
119.474	89.007	195.648	125.953	271.553	167.505	346.698	203.240	387.096	41417.153
122.490	90.571	198.673	127.300	274.506	168.697	349.670	205.226	387.098	42223.680
125.457	92.111	201.678	128.646	277.424	169.840	352.626	206.700	387.110	25998.806
128.490	93.686	204.663	130.004	280.395	171.691	355.716	208.458	387.544	1304.806
131.590	95.380	207.717	131.456	283.342	173.548	358.459	210.775	389.728	233.891
134.647	96.775	210.837	133.092	286.274	175.429	361.641	213.949	392.949	234.741
137.664	98.295	213.937	134.614	289.251	177.992	364.969	216.447	396.074	235.350
140.645	99.756	217.018	135.816	292.277	179.133	368.271	219.209	399.184	236.108
143.690	101.216	220.083	139.061	295.280	180.145	371.065	221.320	402.293	237.054
146.804	102.903	223.124	141.264	298.290	181.316	374.278	223.048		
149.884	104.470	226.123	143.323	301.343	183.527	377.356	225.003		
152.930	105.969	229.086	145.302	304.435	184.830	380.176	228.350		
				Series 2					
343.856	200.316	371.592	220.810	386.989	10815.013	387.075	34102.959	388.402	231.368
346.455	202.231	374.544	223.681	387.029	16380.170	387.076	35195.098	390.881	233.985
349.624	204.759	377.659	225.684	387.034	22189.515	387.079	36240.527	393.331	235.405
352.695	207.191	380.768	227.732	387.055	29851.691	387.084	36435.589	395.774	236.277
355.822	209.438	383.329	231.813	387.049	32262.327	387.083	38426.226	398.220	237.665
359.140	211.212	385.485	286.726	387.067	32933.998	387.088	41347.364		
362.405	212.777	386.559	1371.657	387.063	33492.007	387.091	41400.561		
365.519	215.575	386.888	5139.600	387.068	33516.235	387.096	30361.556		
368.629	217.484	386.962	6332.395	387.071	33642.547	387.148	7294.130		
				Series 3					
342.968	199.879	367.638	216.473	386.936	6848.525	387.084	36166.069	393.172	234.284
345.557	201.092	370.811	219.174	387.006	12239.367	387.090	37994.952	396.353	235.965
348.770	203.519	373.975	222.943	387.037	22330.638	387.091	42313.085	399.522	236.693
351.862	205.789	377.121	225.020	387.055	27054.840	387.095	39501.887	402.678	237.165
354.939	207.376	380.230	226.873	387.061	29775.024	387.098	36490.059		
358.069	209.190	383.211	238.666	387.068	32851.712	387.106	34724.181		
361.258	211.540	385.600	524.541	387.072	34713.898	387.697	886.125		
364.461	214.961	386.719	2987.469	387.075	35214.906	389.989	232.725		

[a] Molar mass $M = 122.17$ g·mol^{-1}.

condensation product collected from DMAP heated to about $T = 550$ K was the same as that of the original sample. Thus we can deduce that DMAP evaporates congruently over the temperature range and completely changes into vapor at 500 K under the present experimental conditions.

Heat Capacity. The experimental molar heat capacities obtained by the adiabatic calorimeter over the temperature range from (80 to 402) K are shown in Figure 3 and tabulated in Table 1. From Figure 3, it can be seen that in the two regions of $T = (80 \text{ to } 382)$ K and $T = (388 \text{ to } 402)$ K the heat capacities of the sample increase in a smooth and continuous manner, respectively; and no phase transition or thermal anomaly occurred. Therefore, the sample is stable in the above temperature range. However, a thermal anomaly was observed in the temperature range from 382 to 388 K with the peak temperature 387.10 K. The thermal anomaly can be ascribed to a solid−liquid phase transition according to the previous thermal analysis.

The molar heat capacities of the sample are fitted to the following polynomial equation of heat capacities ($C_{p,\mathrm{m}}$) with reduced temperature (X) by means of least-square fitting.[25] For the solid phase over the temperature range (80 to 382) K:

$$C_{\mathrm{p,m}}/\mathrm{J{\cdot}K^{-1}{\cdot}mol^{-1}} = 145.61053 + 76.85358X - 0.48674X^2 + 2.79339X^3 - 1.15544X^4 \quad (1)$$

where $X = [(T/\mathrm{K}) - 231]/151$, and T is the absolute temperature. The correlation coefficient of the fitted curve, $R^2 = 0.99907$. The standard deviations of experimental molar heat capacities from the smoothed heat capacities calculated by the polynomial equation were within 0.3 % except for several points around the lower and upper temperature limits. 231 was obtained from half the sum of the upper limit temperature (382 K) and the lower limit temperature (80 K) in the experimental temperature range of (80 to 382) K, and 151 was from half the difference between the upper limit temperature (382 K) and the lower limit temperature (80 K) in the temperature range; the value X is between +1 and −1.

Table 2. Thermodynamic Parameters of the Melting Process Obtained from Three Series of Heat Capacity Measurement

thermodynamic properties	series 1, x_1	series 2, x_2	series 3, x_3	$(-x \pm \sigma_a)^a$
T_m/K	387.091	387.098	387.091	387.094 ± 0.002
$\Delta_{fus}H_m$/kJ·mol^{-1}	21.877	21.630	21.378	21.628 ± 0.144
$\Delta_{fus}S_m$/J·K^{-1}·mol^{-1}	56.516	55.877	55.228	55.873 ± 0.372

[a] $\sigma_a = \sqrt{\sum_{i=1}^{3}(x_i - x)^2/n(n-1)}$, in which n is the experimental number; x_i is a single value in a set of dissolution measurements; and $\bar{x}$ is the mean value of a set of measurement results.

For the liquid phase over the temperature range (388 to 402) K:

$$C_{p,m}/\mathrm{J{\cdot}K^{-1}{\cdot}mol^{-1}} = 235.15628 + 1.44033X - 0.02463X^2 + 0.37907X^3 \quad (2)$$

where $X = [(T/\mathrm{K}) - 395]/7$. The correlation coefficient of the fitted curve, $R^2 = 0.99975$. The standard deviations of experimental molar heat capacities from the smoothed heat capacities calculated by the polynomial equation were within 0.2 %.

Melting Temperature, Enthalpy and Entropy of Fusion. In the phase transition range (from 382 to 388 K), the melting temperature of the sample determined by progressive approach through stepwise heating is given as[26,27]

$$T_m = T_i' + \frac{Q' - \overline{C_0}(T_f - T_i') - nC_{p(L)}(T_f - T_m)}{nC_{p(S+L)}} \quad (3)$$

where T_m is the melting temperature of the sample; T_i' is a certain equilibrium temperature at which solid and liquid phase coexist in the melting region; T_f is a temperature slightly above the melting temperature T_m; Q' is the total heat introduced to heat the sample and the sample cell from T_i' up to T_f: $\overline{C_0}$, the average heat capacity of the empty sample cell in the temperature range from T_i' to T_f; $C_{p(L)}$, the heat capacity of the sample in the liquid region at temperature $(T_f + T_m)/2$; $C_{p(S+L)}$, the heat capacity of the solid–liquid coexistent system at temperature $(T_m + T_i')/2$; n, the number of moles of the sample.

The molar enthalpy of fusion (ΔH_m) of the sample is calculated from the following equation:

$$\Delta_{fus}H_m = \frac{Q - n\int_{T_i}^{T_m} C_{p(S)}\,dT - n\int_{T_m}^{T_i} C_{p(L)} - \int_{T_i}^{T_f} C_0\,dT}{n} \quad (4)$$

where T_i is a temperature point slightly below the starting melting temperature; $C_{p(S)}$ is the heat capacity of the sample in solid region at temperature $(T_i + T_m)/2$; C_0 is the heat capacity of the empty sample cell at temperature $(T_i + T_f)/2$; Q is the total heat introduced to heat the sample and the sample cell from T_i up to T_f.

From molar enthalpy of fusion and the melting temperature, the mole entropy of fusion can be derived by the equation

$$\Delta_{fus}S_m = \frac{\Delta_{fus}H_m}{T_m} \quad (5)$$

The experiment of heat capacity in the fusion region of the sample was carried out three times so that the reversibility and repeatability of the fusion region were verified. Before each series of measurements, the sample was cooled from $T = 400$ K to $T = 300$ K using different cooling rates. In the first series, the sample was quenched into liquid nitrogen (about 20 K·min^{-1}); in the second series, the ice water was used as coolant (about 5 K·min^{-1}); and in the third series, the sample was naturally cooled (about 0.5 K·min^{-1}). The results of the three series of repeated experiments are poltted in the inset to Figure 3 and also given in Table 1.

From the three experiments of heat capacity, melting temperature, molar enthalpy, and molar entropy of fusion were obtained with eqs 3, 4, and 5, respectively. The results are listed in Table 2, and they are in agreement with the results from DSC analysis.

Purity Determination. Adiabatic calorimetry provides an accurate way for determining the purity of a substance in the fusion region of solid–liquid phase transition. The purity of the sample can be evaluated from a set of melting temperatures in the equilibrium of solid–liquid phase transition and melting fractions corresponding to these temperatures.[28,29]

According to the ideal solution law, the relation between the mole fraction N ($N \ll 1$) of a small amount of impurities in the sample and its melting temperature is as follows:

$$N = \frac{\Delta_{fus}H_m(T_0 - T_1)}{RT_0^{\,2}} \quad (6)$$

where T_0 is the melting temperature of an absolutely pure substance; T_1 is the melting temperature of the given sample (strictly speaking, the sample was sealed in the cell, so T_0 and T_1 should be the triple points); ΔH_m is the molar enthalpy of fusion of the sample; and R is the gas constant. As for the liquid solution formed by a part of the sample melted, given that N' is the mole fraction of the impurities and T is the melting temperature of the solution, then N' can be obtained by

$$N' = \frac{\Delta_{fus}H_m(T_0 - T)}{RT_0^{\,2}} \quad (7)$$

Assuming that all the impurities in the sample are solid-insoluble and are transferred completely into the liquid phase when the melting started. Given that m is amount of the impurities; M is the total amount of the sample; M' is the amount of a part of sample melted into liquid solution; F is the ratio of the amount of the sample in the liquid phase to the total amount of the sample, then

$$N = \frac{m}{M} \quad (8)$$

$$N' = \frac{m}{M'} \quad (9)$$

$$F = \frac{M'}{M} \quad (10)$$

From eqs 8 to 10, we obtain

$$N' = \frac{1}{F}N \quad (11)$$

Substituting eqs 6 and 7 into eq 11, we obtain

$$T_0 - T = \frac{1}{F}(T_0 - T_1) \quad (12)$$

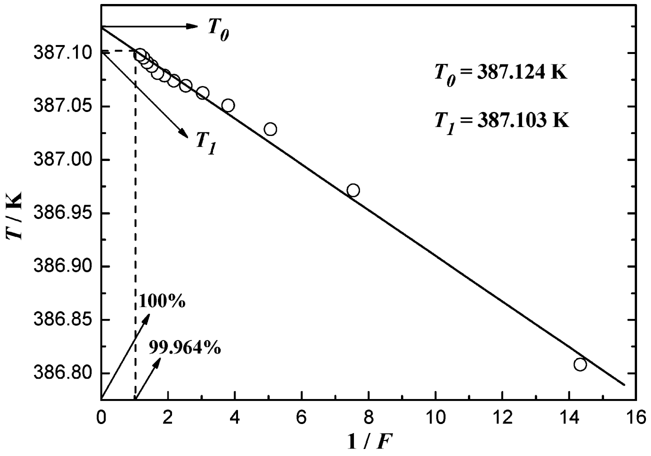

Figure 4. Melting curve (T vs $1/F$) of DMAP.

Table 3. Experimental Results of Melting Fractions F and Equilibrium Temperature T of DMAP

q/J	F	$1/F$	T/K	q/J	F	$1/F$	T/K
46.985	0.0698	14.3294	386.808	354.779	0.5270	1.8977	387.079
89.236	0.1325	7.5448	386.971	399.260	0.5930	1.6863	387.081
132.892	0.1974	5.0663	387.029	443.723	0.6591	1.5173	387.088
177.088	0.2630	3.8019	387.051	488.273	0.7252	1.3789	387.091
221.443	0.3289	3.0404	387.063	532.817	0.7914	1.2636	387.096
265.889	0.3949	2.5321	387.069	577.374	0.8576	1.1661	387.098
310.310	0.4609	2.1697	387.074				

F is also designated as the fraction melted, its value being the ratio of the heat required to melt a part of the sample q to the total heat required to melt the whole sample Q, then we have

$$F = \frac{q}{Q} \tag{13}$$

The heat q introduced to the sample can be measured by the adiabatic calorimeter, and $Q = n\cdot\Delta_{\text{fus}}H_{\text{m}}$, so F can be determined.

Equation 12 suggests that the relationship between the equilibrium melting temperature T and the reciprocal of melting fraction $1/F$ is linear. By plotting T versus $1/F$ and extrapolating the straight line to $1/F = 1$ and $1/F = 0$, T_1 and T_0 can be derived. The results are tabulated in Table 3 and plotted in Figure 4, where T_1 =387.106 K and T_0 = 387.127 are obtained. The melting temperature (T_1 = 387.106 K) agrees well with that (T_{m} = 387.094 ± 0.002 K) obtained from the heat capacity measurements as described earlier. From eq 4, N = 0.000363 mole is evaluated. The mole fraction purity of the sample is 1 − N = 99.946 %.

Thermodynamic Functions. The thermodynamic functions relative to the reference temperature 298.15 K were calculated in the temperature range (80 to 380) K and (390 to 400) K with an interval of 5 K, using the polynomial equation for heat capacity and thermodynamic relationships as follows:

Before the melting of the sample,

$$H_{\text{T}} - H_{298.15} = \int_{298.15}^{T} C_{\text{p,m}}(\text{S})\,\text{d}T \tag{14}$$

$$S_{\text{T}} - S_{298.15} = \int_{298.15}^{T} C_{\text{p,m}}(\text{S})/T\,\text{d}T \tag{15}$$

After the melting of the sample,

$$H_{\text{T}} - H_{298.15} = \int_{289.15}^{T_i} C_{\text{p,m}}(\text{S})\,\text{d}T + \Delta_{\text{fus}}H_{\text{m}} + \int_{T_i}^{T} C_{\text{p,m}}(\text{L}) \tag{16}$$

$$S_{\text{T}} - S_{298.15} = \int_{298.15}^{T_{\text{i}}} [C_{\text{p,m}}(\text{S})/T] + \frac{\Delta_{\text{fus}}H_{\text{m}}}{T_{\text{m}}} + \int_{T_{\text{f}}}^{T} [C_{\text{p,m}}(\text{L})/T]\,\text{d}T \tag{17}$$

The values of thermodynamic function $H_T - H_{298.15}$ and $S_T - S_{298.15}$ are listed in Table 4.

Constant-Volume Combustion Energy, Standard Molar Enthalpy of Combustion, and Standard Enthalpy of Forma-

Table 4. Calculated Thermodynamic Function Data of DMAP

T	C_p	$H_T - H_{298.15}$	$S_T - S_{298.15}$	T	C_p	$H_T - H_{298.15}$	$S_T - S_{298.15}$	T	C_p	$H_T - H_{298.15}$	$S_T - S_{298.15}$
K	$\text{J}\cdot\text{K}^{-1}\cdot\text{mol}^{-1}$	$\text{kJ}\cdot\text{mol}^{-1}$	$\text{J}\cdot\text{K}^{-1}\cdot\text{mol}^{-1}$	K	$\text{J}\cdot\text{K}^{-1}\cdot\text{mol}^{-1}$	$\text{kJ}\cdot\text{mol}^{-1}$	$\text{J}\cdot\text{K}^{-1}\cdot\text{mol}^{-1}$	K	$\text{J}\cdot\text{K}^{-1}\cdot\text{mol}^{-1}$	$\text{kJ}\cdot\text{mol}^{-1}$	$\text{J}\cdot\text{K}^{-1}\cdot\text{mol}^{-1}$
					Crystal						
80	66.632	−27.018	−147.083	185	122.084	−17.086	−71.007	290	175.759	−1.450	−4.933
85	69.332	−26.678	−142.981	190	124.657	−16.469	−67.723	295	178.347	−0.564	−1.904
90	72.026	−26.324	−138.948	195	127.226	−15.839	−64.458	298.15	179.982	0.000	0.000
95	74.716	−25.957	−134.979	200	129.790	−15.197	−61.209	300	180.944	0.334	1.117
100	77.400	−25.577	−131.071	205	132.350	−14.541	−57.976	305	183.552	1.245	4.130
105	80.079	−25.183	−127.219	210	134.906	−13.873	−54.759	310	186.172	2.169	7.135
110	82.752	−24.776	−123.422	215	137.458	−13.192	−51.557	315	188.804	3.107	10.133
115	85.419	−24.356	−119.674	220	140.008	−12.499	−48.368	320	191.451	4.057	13.125
120	88.080	−23.922	−115.973	225	142.556	−11.792	−45.193	325	194.112	5.021	16.110
125	90.735	−23.475	−112.316	230	145.102	−11.073	−42.030	330	196.789	5.999	19.089
130	93.383	−23.015	−108.700	235	147.646	−10.341	−38.880	335	199.485	6.989	22.064
135	96.024	−22.541	−105.123	240	150.190	−9.597	−35.741	340	202.198	7.993	25.033
140	98.659	−22.055	−101.582	245	152.734	−8.839	−32.614	345	204.932	9.011	27.999
145	101.287	−21.555	−98.075	250	155.279	−8.069	−29.498	350	207.688	10.043	30.962
150	103.909	−21.042	−94.600	255	157.825	−7.287	−26.393	355	210.466	11.088	33.923
155	106.524	−20.516	−91.154	260	160.374	−6.491	−23.298	360	213.269	12.148	36.882
160	109.133	−19.976	−87.736	265	162.925	−5.683	−20.213	365	216.097	13.221	39.842
165	111.735	−19.424	−84.345	270	165.481	−4.862	−17.139	370	218.953	14.309	42.802
170	114.331	−18.859	−80.977	275	168.041	−4.028	−14.074	375	221.837	15.411	45.764
175	116.921	−18.281	−77.633	280	170.607	−3.181	−11.018	380	224.752	16.527	48.731
180	119.505	−17.690	−74.310	285	173.179	−2.322	−7.971				
					Liquid						
390	233.977	39.578	108.314	400	236.311	41.930	114.268				
395	235.156	40.751	111.303	405	238.269	43.116	117.214				

Table 5. Experimental Results of the Combustion Energy of DMAP Obtained from the Oxygen-Bomb Combustion Calorimetry at T = 298.15 K

no.	sample mass, m/g	heat value of nickel wire, Q_{Ni}/J	heat value of nitric acid, Q_N/J	corrected temperature rise, ΔT/K	combustion energies, ΔU_c/kJ·mol^{-1}
1	0.39444	39.539	38.426	0.97466	4229.96
2	0.40856	39.685	41.542	1.01013	4232.28
3	0.41006	40.857	45.696	1.01454	4233.71
4	0.41351	39.978	42.996	1.02267	4233.31
5	0.41364	34.853	44.917	1.02250	4232.22
6	0.41359	40.417	39.984	1.02194	4230.18
7	0.41574	40.125	44.658	1.02838	4233.72

[a] Averge $\Delta U_c = -(4232.20 \pm 0.60)$ kJ·mol^{-1}.

tion. The constant-volume combustion energy can be calculated from the equation:

$$\Delta_c U = (\epsilon_{calor} \cdot \Delta T - Q_{Ni} - Q_{HNO3}) \cdot M/W \qquad (18)$$

in which ϵ_{calor} was the energy equivalent of the oxygen bomb calorimeter; ΔT was the corrected temperature rise; M was the molar mass of the sample; and W was the mass of the sample. The results calculated by the equation are listed in Table 5. The standard molar enthalpy of combustion, $\Delta_c H_m^0$, referred to the combustion enthalpy change of the following reaction at T = 298.15 K and P^0 = 100 kPa based on the definition of the combustion enthalpy about the organic compound:

$$C_7H_{10}N_2(cr) + 19/2O_2(g) = 7CO_2(g) + 5H_2O(l) + N_2(g) \qquad (19)$$

The standard molar enthalpies of combustion can be derived from the constant-volume combustion energy by means of the following formula:

$$\Delta_c H_m{}^0 = \Delta_c U_m + \Delta n \cdot RT \qquad (20)$$

$$\Delta n = \Sigma n_i(\text{products, g}) - \Sigma n_i(\text{reactants, g}) \qquad (21)$$

where Σn_i was the total molar amount of the gases in products or reactants. The calculated standard molar enthalpy of combustion was $\Delta_c H_m^0 = -(4235.92 \pm 0.60)$ kJ·mol^{-1}.

The standard molar enthalpy of formation, $\Delta_f H_m^0$, was calculated by a designed Hess thermochemical cycle according to eq 19 as follows:

$$\Delta_f H_m{}^0(C_7H_{10}N_2, cr) = [7\Delta_f H_m{}^0(CO_2, g) + 5\Delta_f H_m{}^0(H_2O, l)] - \Delta_c H_m{}^0(C_7H_{10}N_2, cr) \qquad (22)$$

In the above formula, the standard molar enthalpies of formation of CO_2(g) and H_2O(l) recommended by CODATA,[30,31] $\Delta_f H_m^0(CO_2, g) = -(393.51 \pm 0.13)$ kJ·mol^{-1}, and $\Delta_f H_m^0(H_2O, l) = -(285.83 \pm 0.04)$ kJ·mol^{-1}, were employed in the calculation of $\Delta_f H_m^0(C_7H_{10}N_2, cr)$ values. Based on these values and the standard molar enthalpy of combustion, the standard molar enthalpy of formation can be calculated to be $\Delta_f H_m^0(C_7H_{10}N_2, cr) = (52.20 \pm 1.71)$ kJ·mol^{-1}.

Conclusion

The heat capacities of DMAP were measured in the temperature range from (80 to 402) K by a high-precision automated adiabatic calorimeter. From the results of heat capacity experiment, the thermodynamic properties of fusion range from (382 to 388) K were completely studied, and the thermodynamic functions $[H_T - H_{298.15}]$ and $[S_T - S_{298.15}]$ were derived in the range from (80 to 400) K with temperature intervals of 5 K. The melting temperature T_m, the molar enthalpy $\Delta_{fus}H_m$, and the entropy $\Delta_{fus}S_m$ of fusion were determined to be (387.094 ± 0.002) K, (21.628 ± 0.144) kJ·mol^{-1}, and (55.873 ± 0.372) J·K^{-1}·mol^{-1}, respectively. The mole fraction purity was calculated to be 0.99964 according to the van't Hoff equation. The standard molar enthalpy of formation of DMAP was derived to be (52.20 ± 1.71) kJ·mol^{-1} with a precision oxygen-bomb combustion calorimeter.

Literature Cited

(1) Kumar, M.; Singh, S. K.; Agarwal, A. Production of 4-dimethyl amino pyridine e.g. catalyst in acylation reaction comprises quaternizing pyridine in presence of organic solvent and then aminating product. U.S. Patent 2004106801-A1, 2004.

(2) Steglich, W.; Höfle, G. *N*,*N*-Dimethyl-4-pyridinamine, a very effective acylation catalyst. *Angew. Chem. Int. Ed. Engl.* **1969**, *8*, 981−981.

(3) Höfle, G.; Steglich, W.; Vorbrüggen, H. 4-Dialkylaminopyridines as highly active acylation catalysts. [New synthetic method (25)]. *Angew. Chem. Int. Ed. Engl.* **1978**, *17*, 569−583.

(4) Scriven, E. F. V. 4-Dialkylaminopyridines: super acylation and alkylation catalysts. *Chem. Soc. Rev.* **1983**, *12*, 129−161.

(5) Murugan, R.; Scriven, E. F. V. Applications of dialkylaminopyridine (DMAP) catalysts in organic synthesis. *Aldrichim. Acta* **2003**, *36*, 21−28.

(6) Price, K. E.; Mason, B. P.; Bogdan, A. R.; Broadwater, S. J.; Steinbacher, J. L.; McQuade, D. T. Microencapsulated linear polymers: "soluble" heterogeneous catalysts. *J. Am. Chem. Soc.* **2006**, *128*, 10376−10377.

(7) Murayama, M.; Sanda, F.; Endo, T. Anionic ring-opening polymerization of a cyclic carbonate having a norbornene structure with amine initiators. *Macromolecules* **1998**, *31*, 919−923.

(8) Dell'Erba, I. E.; Williams, R. J. J. Homopolymerization of epoxy monomers initiated by 4-(dimethylamino)pyridine. *Polym. Eng. Sci.* **2006**, *46*, 351−359.

(9) Gittins, D. I.; Caruso, F. Spontaneous phase transfer of nanoparticulate metals from organic to aqueous media. *Angew. Chem. Int. Ed.* **2001**, *40*, 3001−3004.

(10) Gandubert, V. J.; Lennox, R. B. Assessment of 4-(dimethylamino)-pyridine as a capping agent for gold nanoparticles. *Langmuir* **2005**, *21*, 6532−6539.

(11) Bappert, E.; Müller, P.; Fu, G. C. Asymmetric [3 + 2] annulations catalyzed by a planar-chiral derivative of DMAP. *Chem. Commun.* **2006**, *24*, 2604−2606.

(12) Busto, E.; Gotor-Fernández, V.; Gotor, V. Biocatalytic preparation of optically active 4-(*N*,*N*-dimethylamino)pyridines for application in chemical asymmetric catalysis. *Tetrahedron: Asymmetry* **2006**, *17*, 1007−1016.

(13) Fu, G. C. Asymmetric catalysis with "planar-chiral" derivatives of 4-(dimethylamino)pyridine. *Acc. Chem. Res.* **2004**, *37*, 542−547.

(14) Anderson, L. C.; Seeger, N. V. The absorption spectra of the aminopyridines. *J. Am. Chem. Soc.* **1949**, *71*, 340−342.

(15) Dastidar, P.; Guru Row N. T.; Prasad, B. R.; Subramanian, C. K.; Bhattacharya, S. Binary salts of substituted pyridines and L-tartaric acid as nonlinear optical organic materials: crystal structure of L-tartaric acid−4-dimethylaminopyridine (1:1) dehydrate salt. *J. Chem. Soc. Perkin Trans. 2* **1993**, 2419−2412.

(16) Tan, Z. C.; Sun, L. X.; Meng, S. H.; Li, L.; Zhang, J. B. Heat capacities and thermodynamic functions of *p*-chlorobenzoic acid. *J. Chem. Thermodyn.* **2002**, *34*, 1417−1429.

(17) Tan, Z. C.; Sun, G. Y.; Sun, Y.; et al. An adiabatic low-temperature calorimeter for heat capacity measurement of small samples. *J. Therm. Anal.* **1995**, *45*, 59−67.

(18) Tan, Z. C.; Sun, G. Y.; Song, Y. J.; Wang, L.; Han, J. R.; Liu, Y. S.; et al. An adiabatic for heat capacity measurement of small samples— The heat capacity of nonlinear optical materials $KTOPO_4$ and $RbTiOAsO_4$ crystals. *Thermochim. Acta* **2000**, *252−253*, 247−253.

(19) Archer, D. G. Thermodynamic properties of synthetic sapphire (α-Al_2O_3), standard reference material 720 and the effect of temperature-scale differences on thermodynamic properties. *J. Phys. Chem. Ref. Data* **1993**, *22*, 1441−1453.

(20) Di, Y. Y.; Tan, Z. C.; Sun, X. H.; Wang, M. H.; Xu, F.; Liu, Y. F.; Sun, L. X.; Zhang, H. T. Low-temperature heat capacity and standard molar enthalpy of formation of 9-fluorenemethanol ($C_{14}H_{12}O$). *J. Chem. Thermodyn.* **2004**, *36*, 79−86.

(21) Zhang, L. M.; Tan, Z. C.; Wang, S. D.; Wu, D. Y. Combustion calorimetric and thermogravimetric studies of graphite and coals dopes with a coal-burning additive. *Thermochim. Acta* **1997**, *299*, 13−17.

(22) Wu, X. M.; Tan, Z. C.; Meng, S. H.; Sun, C. X.; Wang, F. D.; Qu, S. S. Study on thermodynamic properties of polypyromellitimide molding power. *Thermochim. Acta* **2000**, *359*, 103−107.

(23) Aguilar, A. R.; Guareno, E. O. Thermochemistry of methyl-D-glucopyranosides and methyl-D-galactopyranosides. *J. Chem. Thermodyn.* **2000**, *32*, 767−775.
(24) Melkhanova, S. V.; Pimenova, S. M.; Kolesov, V. P.; Pimerzin, A. A.; Sarkisova, V. S. The standard molar enthalpies of formation of some alkyladamantanes. *J. Chem. Thermodyn.* **2000**, *32*, 1311−1317.
(25) Andrews, J. T. S.; Norton, P. A.; Westrum, E. F., Jr. An adiabatic calorimeter for use at superambient temperatures. The heat capacity of synthetic sapphire (α-Al_2O_3) from 300 to 550 K. *J. Chem. Thermodyn*. **1978**, *10*, 949−958.
(26) Tan, Z. C.; Ye, J. C.; Yin, A. X.; Chen, S. X.; Wang, W. B. Heat capacity and thermodynamic properties of 2-chloro-6-(trichloromethyl)pyridine. *Chin. Sci. Bull.* **1987**, *32*, 240−246.
(27) Di, Y. Y.; Tan, Z. C.; Wu, X. M.; Meng, S. H.; Qu, S. S. Heat capacity and thermochemical study of trifluoroacetamede ($C_2H_2F_3NO$). *Thermochim. Acta* **2000**, *356*, 143−151.
(28) Zhang, Z. Y.; Frenkel, M.; et al. *Thermodynamic Properties of Organic Compounds and their Mixtures*, Group IV, Vol. 8, Subvolume A; Springer: Berlin, 1995; Chaper 7.
(29) Badley, J. H. The calorimetric determination of purity-theory and calculation methods. *J. Phys. Chem.* **1959**, *63*, 1991−1996.
(30) Cox, J. D.; Wagman, D. D.; Medvedev, V. A. *CODATA*; Hemisphere: New York, 1989.
(31) Cox, J. D. CODATA recommended key values for thermodynamics, 1977 report of the CODATA task group on key values for thermodynamics, 1977. *J. Chem. Thermodyn.* **1978**, *10*, 903−906.

Received for review November 28, 2006. Accepted February 1, 2007. The authors gratefully acknowledge the National Natural Science Foundation of China for financial support of this work under NSFC Grant 20373072.

JE6005423